

Numerical Simulation of the Effect of Valve Opening and Particle Concentration on the Erosion Damage in Ball Valves of Pressure Reducing Station

Amir Askari, Ali Falavand Jozaei *

Department of Mechanical Engineering, Ahvaz Branch, Islamic Azad University, Ahvaz, Iran

ARTICLE INFO

Article history:

Received 07 March 2018

Accepted 25 April 2018

Keywords:

Ball valve

Erosion

Particle concentration

Valve opening

Simulation

ABSTRACT

Ball valve is one of valves that have many applications in industry especially in gas delivery systems. This kind of valve is categorized in the on- off flow control valve. This study aims to investigate unusual application of ball valve to control fluid flow in the oil and gas industry and its destructive effect including erosion of ball and body of valve. Simulation of industrial ball valve is done using ANSYS Fluent software and effect of erosion on it is investigated in different working conditions. In this study, working condition is performed regarding 3 different concentrations for suspended particles as well as four positions of ball in different angles. It is shown that rate of erosion for 25% open state of valve is increased to about 15000 times of complete open state of valve, and rate of erosion is increased to about 3500 times for half open state (50% open state); and rate of erosion is increased to about 220 times for 75% open state of valve.

1. Introduction

In ball valve the flow blocker is a spherical or half- spherical member which rotates 90 degree by stem around a vertical axis with regard to the direction of fluid. On the sphere, a hole is embedded. If the hole is open, it is in the direction of the flow channel and when closed, it is perpendicular to the path. When the ball is in the state other than above mentioned state, turbulent flow is made in the valve. This limits the application of ball valve and causes problems such as erosion. Researches carried out at out erosion are as follows:

Haugen et al. [1] studied erosion on choke valves and showed that erosion can be reduced by selecting durable materials and optimizing the design. They selected and investigated 28 different materials. McLaury et al. [2] employed the API RP 14E method to study erosion and the methods used for its limitation. Forder et al. [3] investigated erosion in control valves and showed that in addition to erosion, presence of suspended solid particles in the fluid causes the valve to lose its controlling capabilities. Parslow et al. [4] studied erosion in a tee caused by presence of solid particles and reported that factors such as the number of particles, velocity, and particles collision angle can control erosion. In their study, Kavner et al. [5] investigated the phase stability and density of FeS at different pressures and temperatures. Jin et al. [6] carried out erosion numerical simulation in tube due to particle collision in which useful results such as redundancy distribution of particle collision and erosion of tube were obtained. Oka et al. [9] showed that intensity of erosion is affected by the compactness and pulses of suspended particles and proved that the velocity and collision angle of

particles significantly affect corrosion erosion. Habib et al. [11] investigated erosion in heat exchangers and assessed the effect of flow velocity and particle sizes on erosion. They proved that erosion rate is related to the particles velocity and particle size in erosion is significant. Malka et al. [12] showed that erosion leads to corrosion and wear, while corrosion and erosion increase wear. Shahbazi and Noori zadeh [19] conducted studies on the black powder present in natural gas transmission network and introduced the ingredients of this powder using different techniques and methods. Shafee et al. [20] used CFD to numerically analyze erosion in pipelines and gas stations. Zhu et al. [21] assessed erosion in needle valves and investigated the effect of factors such as fluid inlet velocity, concentration, diameter and shape of particles on erosion. They believed that valve lifetime can be extended by altering the shape of particles or their velocity at the inlet. Moreover, they suggested that changing the diameter of particles has the most significant effect on erosion reduction. Droubi et al. [22] studied erosion caused by collision of suspended particles in elbow and showed that factors such as equipment shape, flow conditions, and suspended particles play a significant role in erosion. Flow erosion is a highly complicated issue due to a number of parameters including operation, structure and fluid parameters affecting the erosion severity, such as flow velocity, flow channel structure, fluid properties, particle diameter and particle concentration [10], [14]. Fan et al. [7], Suzuki et al. [13], Tang et al [14], Li et al. [16] and Yan et al. [17] investigates has been carried out in attempts to explain flow erosion by physical or numerical modeling. Zhang et al. [18] conducted numerical investigation of the location of maximum erosive wear damage in elbow. Deng et al. [8] carried out experiments with four bend orientations to

* Corresponding author. Tel.: +98-91-6610-3732; fax: + 98-61-3334-8356; e-mail: falavand@iauhvaz.ac.ir

investigate the effect of bend orientation on puncture point location. Ferng and Lin [15] pointed out that the geometry of flow channel presents obvious effect on flow erosion. However, the majority of these investigations focus on the erosion of pipe bends elbows and tees whereas limited number of them has been conducted on valves. Specifically, no studies were conducted on erosion in ball valves.

2. Explanation of Problem

Let 's consider a ball valve with internal diameter of 400 mm and length of assembly up to two flange heads equal to 762 mm. In order to prevent reverse flow, solution range is elongated 1 meter from each side. Valve is simulated with rotation of ball in

four open conditions including complete open, half- open, 75% open and 25% open states, and two concentrations are arranged for every state. Working fluid along with solid particles enters a valve from one side, and after passing through the path, hitting the ball, and making erosion, it leaves the valve from other side. Working fluid is defined as compressible one according to laws and rules for ideal gas. Suspended FeS particles are inert and spherical. While using uniform model for each state the distribution of particles with three different diameters (3.86 μm , 267.45 μm and 531.03 μm) [18] are chosen and then rate of erosion is calculated.

Table 1. Simulation cases

	V(m/s)	valve opening	\dot{m} particle(kg/s)	Case	Operation condition
				P_{in} (bar)	P_{out} (bar)
1	13	1.00	0.0395 -3%	28.19	27.94
2	13	1.00	0.0798 -6%	28.19	27.94
3	13	1.00	0.1184 -9%	28.19	27.94
4	16	0.75	0.0362 - 3%	28.19	27.9
5	16	0.75	0.0724 - 6%	28.19	27.9
6	16	0.75	0.1086 - 9%	28.19	27.9
7	23	0.50	0.0348 - 3%	28.19	27.7
8	23	0.50	0.0696 - 6%	28.19	27.7
9	23	0.50	0.104 - 9%	28.19	27.7
10	45	0.25	0.0333 - 3%	28.19	25.9
11	45	0.25	0.0665 - 6%	28.19	25.9
12	45	0.25	0.0998 - 9%	28.19	25.9

Table 2. Physical and mechanical properties for particle and valve

Density of Fes (kg/m ³)	Roughness of Valve (mm)	Diameter of particle (μm)		
		min	mean	max
5960 [5]	0.05	3.87	267.45	531.03

3. Governing Equations and Numerical Method

3.1. Governing Equations

Three main steps are involved in CFD-based erosion:

Flow modeling, particle tracking, erosion computation. First, gas is seemed as continuous fluid phase evaluated by a Navier–Stokes solver, and solid particles are treated as spherical particles with uniform diameter added into continuous phase flow field as discrete phase, which are captured by discrete phase model (DPM). And particles are inert are assumed in simulation.

The mass and momentum conservation equations used in the continuous fluid flow model are given in Eqs. (1) and (2), respectively [21]:

$$\nabla \times (\rho_f \mathbf{v}) = 0 \quad (1)$$

$$\nabla \times (\rho_f \mathbf{v} \mathbf{v} - \boldsymbol{\tau}_f) = f_f \quad (2)$$

In which,

$$\boldsymbol{\tau}_f = \left[-p + \left(-g - \frac{2}{3} \mu \right) \nabla \times \mathbf{v} \right] \mathbf{I} + 2\mu \mathbf{E} \quad (3)$$

$$E = \frac{1}{2} \nabla \mathbf{v} + \nabla \mathbf{v}^T \quad (4)$$

Where \mathbf{V} is velocity of gas, ρ_f is density of gas, f_f is volume force of fluid, $\boldsymbol{\tau}_f$ is stress of fluid, P is pressure, μ is dynamic viscosity, \mathbf{I} is second order unit tensor and \mathbf{g} is gravitational acceleration. In addition, for equations of k- ϵ turbulence model [21]:

$$\frac{\partial \rho_f k v_i}{\partial X_i} = \frac{\partial}{\partial X_j} \left[\left(\mu + \frac{\mu_t}{\sigma_k} \right) \frac{\partial k}{\partial X_j} \right] + G_k + G_b - \rho_f \epsilon - Y_M \quad (5)$$

$$\frac{\partial \rho_f \epsilon v_i}{\partial X_i} = \frac{\partial}{\partial X_j} \left[\left(\mu + \frac{\mu_t}{\sigma_\epsilon} \right) \frac{\partial \epsilon}{\partial X_j} \right] + \rho_f C_1 S \epsilon - \rho_f C_2 \frac{\epsilon^2}{K + \sqrt{v \epsilon}} + c_{1\epsilon} \frac{\epsilon}{K} C_{3\epsilon} G_b \quad (6)$$

$$\rho_f C_2 \frac{\epsilon^2}{K + \sqrt{v \epsilon}} + c_{1\epsilon} \frac{\epsilon}{K} C_{3\epsilon} G_b$$

In which,

$$C_i = \max \left(0.43, \frac{\eta}{\eta + 5} \right) \quad (7)$$

$$\eta = 2S_{ij} \times S_{ij}^{\frac{1}{2}} \frac{K}{\varepsilon} \quad (8)$$

$$S_{ij} = \frac{1}{2} \left(\frac{\partial v_i}{\partial X_j} + \frac{\partial v_j}{\partial X_i} \right) \quad (9)$$

Where the subscripts i and j indices for coordinate axes, k and ε refer to turbulent kinetic energy and turbulent kinetic energy dissipation rate per unit mass, respectively, σ_k and σ_ε present Prandtl number corresponding to turbulent kinetic energy and Prandtl number corresponding to turbulent kinetic energy dissipation rate, respectively. Y_m is impact of compressible turbulence inflation on the total dissipation rate, ν is molecule kinetic viscosity, G_k is production term of turbulent kinetic energy due to the average velocity gradient, G_b is production term of turbulent kinetic energy due to lift and C_{12} , C_2 and C_{32} are empirical constants taken as 1.44, 1.9 and 0.09, respectively [21]. After continuous phase flow field such as velocity and pressure distribution obtained by solving the above equations, the particle dynamics are treated in a Lagrangian framework according to the particle equation of motion, including the trajectory of particles, the attack angle and velocity perturbation [21]. This particle motion equation is called as DPM model and is specified as

$$\frac{dv_s}{dt} = \frac{C_D Re_{ds}}{24\tau_t} v - v_s + \frac{g(\rho_s - \rho_f)}{\rho_s} + 0.5 \frac{\rho_f}{\rho_s} \frac{d}{dt} (v - v_s) \quad (10)$$

In which,

$$\tau_t = \frac{\rho_s d_s^2}{18\mu} \quad (11)$$

$$Re_{ds} = \frac{\rho_f d_s |v_s - v|}{\mu} \quad (12)$$

$$C_D = \frac{24}{Re_{ds}} \left(1 + b_1 Re_{ds}^{b_2} + \frac{b_3 Re_{ds}}{b_4 + Re_{ds}} \right) \quad (13)$$

Where ρ_s is density of particle, d_s is diameter of particle, v_s is velocity of particle, Re_{ds} is particle equivalent Reynolds number, C_D is drag coefficient, τ_t is particle relaxation time, b_1 , b_2 , b_3 and b_4 are constants taken as 0.186, 0.653, 0.437 and 7178.741, respectively. We can simply write the DPM relation without considering the effect of gravity:

$$\frac{d\vec{u}_p}{dt} = F_D \vec{u} - \vec{u}_p \quad (14)$$

In which,

$$F_D = \frac{18\mu_m C_D Re}{\rho_p d_p^2} \quad (15)$$

The force that was exerted on the secondary phase is drag force that was exerted by fluid, and value of C_D coefficient is a function of Reynolds number. If the particle shape is considered spherical [22], we have:

$$C_D = a_1 + \frac{a_2}{Re} + \frac{a_3}{Re^2} \quad (16)$$

In order to calculate the rate of erosion, we can use mathematical model that makes the effect of above-mentioned different parameters dependent on the rate of erosion. The mathematical model and its inner parameters are as follows

$$ER = \frac{\sum_{p=1}^{N_{particles}} C_d V^n f \alpha \dot{m}}{A_{face}} \quad (17)$$

Where ER is mass of material loss per unit area per unit time, C_d is Particle diameter function, V is Particle impact velocity, n is Velocity exponent, f (α) is impact angle function and \dot{m} is Particle mass flow rate.

3.2. Numerical Method

Simulation of above equations could be done by using ANSYS Fluent 15 software which covers all models and related equations. Numerical method used in this software is finite volume according to which we should produce the computational mesh in the proper range and solve the above equations with proper boundary conditions. This software allows the designer to define all parameters of fluid material as well as properties of particles. The type of solver used in this problem is steady state with simple algorithm without considering the gravity effect. Furthermore, second-order upwind with acceptable accuracy is used for spatial discretization.

3.3 Computational Mesh

The generated mesh is chosen as a hybrid type the cells near to wall are prism type and has inflation layers and growth factor to calculate boundary layer while the cells far from wall are tetra type. To establish such mesh (three layers) and growth factor of 1.1 are used (figure 1).

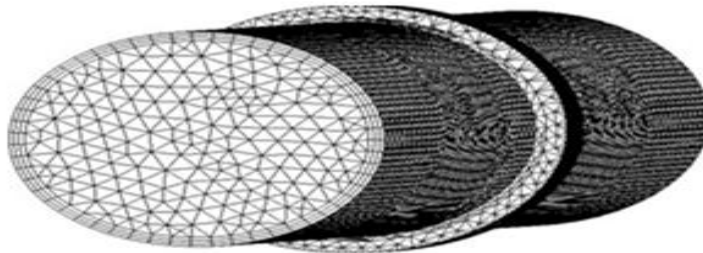


Figure 1. diagram of mesh

Analysis is done in seven steps due to independence of mesh. When the number of mesh is increased at each step, the rate of erosion is calculated. In the last step, rate of error is decreased to 0.821 that is shown in the figure 2.

4. Validation

In order to verify the flow modelling capabilities, a verification study is performed on a 90° elbow with the specific

parameters used are shown in Table 3. By comparing the predicted erosion rate with the published work of Droubi [22], the accuracy of the flow solution can be assessed. The shape of the contour plots of erosion. The similarities in the erosion profiles illustrate that the results collated in the test cases will provide valid qualitative data to analysis erosion.

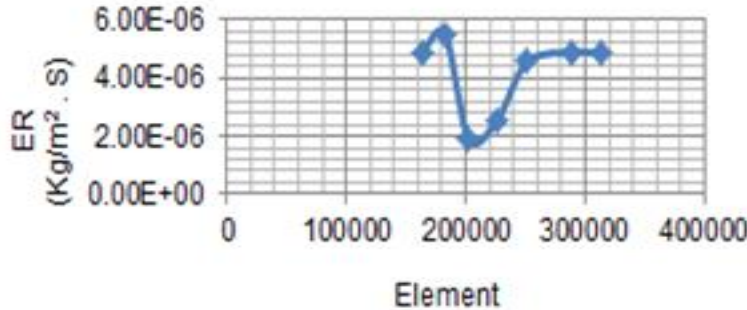


Figure 2. diagram of Computational mesh

Table 3. Validation Test Parameters

Pipe Diameter (m)	Bend Radius (m)	Carrier Fluid Velocity (m/s)	Carrier Fluid	Particle Diameter (m)	Particle Density (kg/m ³)	Sand Production Rate (kg/day)
0.0508	1.5D	15.24	Methane	150 μm	2650	4.55

Rate of erosion is drawn after arrangement and solution.

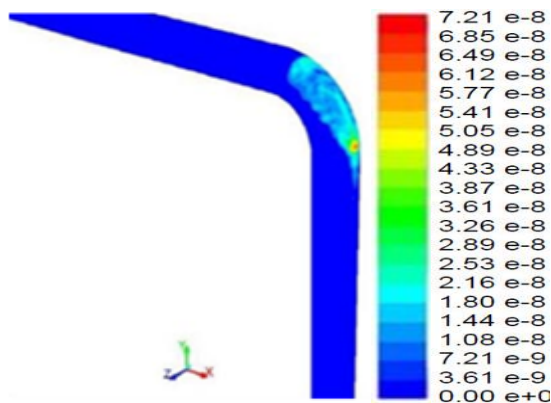


Figure.3a.contour of ER by Droubi

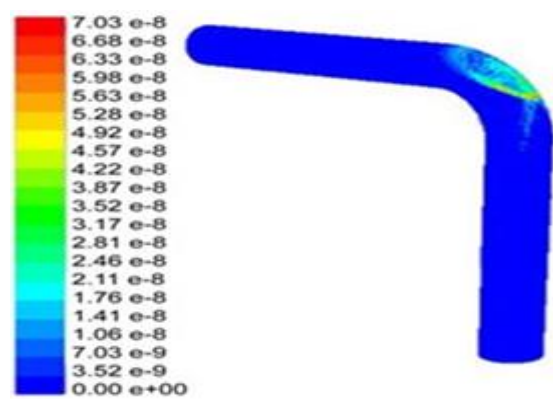


Figure.3b. contour of ER for validation

The erosion rate was calculated 7.21×10^{-8} (kg/m².s) by Droubi (Figure.3a) [22] and the amount of erosion rate acquired 7.03×10^{-8} (kg/m².s) in this research (Figure.3b). The obtained results are in agreement with analyses done for validation and its rate of error is less than 2.5%.

5. Results

The results are investigated in terms of some aspects.

5.1. The effect of valve opening

5.1.1. Particle concentration: 3%

In figures 4 a, b, and c, velocity increases occurs in position after the ball. This occurs due to reduction in cross- section and occurrence of turbulence. Figure d shows complete

openness of valve. The speed is constant in all parts due to lack of change in cross- section.

In three states of a, b, and c in figure 5, there is impact erosion that is done due to collision of particles and their reflection. But in state of d due to complete openness of valve, the effect of erosion is just sliding erosion and its area get out of centralization and it is scattered in the environment. The most rate of erosion occurs in the state of a.

Investigating the results of each state by standard condition that is complete open state of valve is as follows:

- In the 25% open state, rate of erosion is increased to 15800.
- In the 50% open state, rate of erosion is increased to 3830.
- In the 75% open state, rate of erosion is increased to 226.

This shows an increase in rate of erosion and thus serious destruction of valve.

5.1.2. Particle concentration: 6%

It is observed that range of results is the same as previous step. There are impact erosions in three steps and sliding erosion in state of d (figure 6). Investigating the results of each state by standard condition that is complete open state of valve is as follows:

- In the 25% open state, rate of erosion is increased to 15600.
- In the 50% open state, rate of erosion is increased to 344.
- In the 75% open state, rate of erosion is increased to 217.

And again shows an increase in rate of erosion and thus serious destruction of valve.

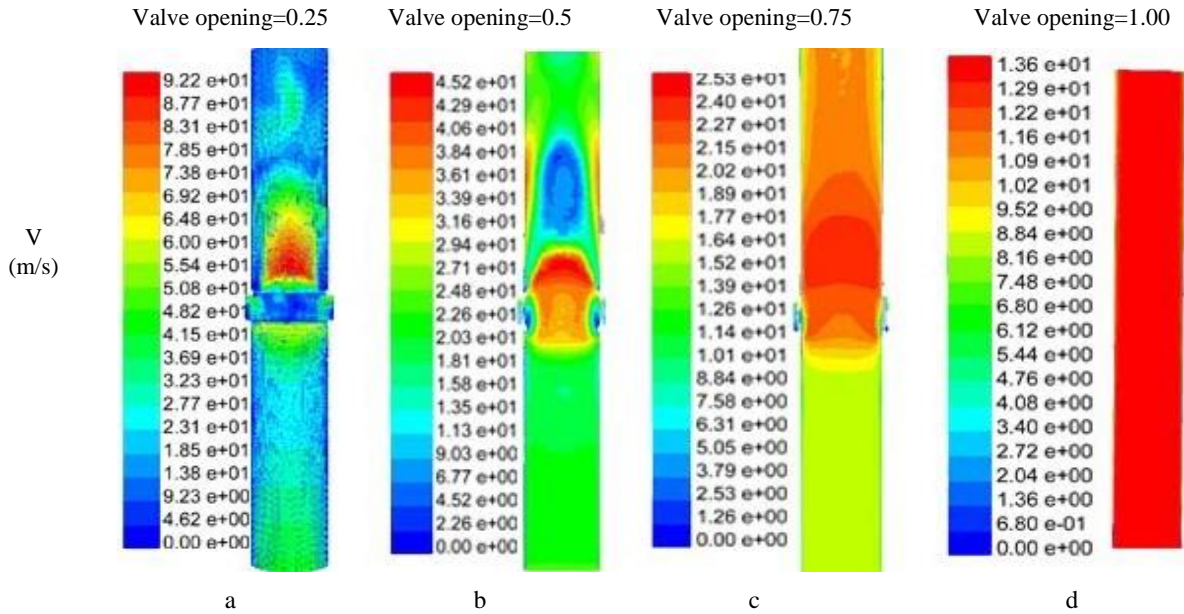


Figure.4. Effects of valve opening on velocity for 3% of particle concentration

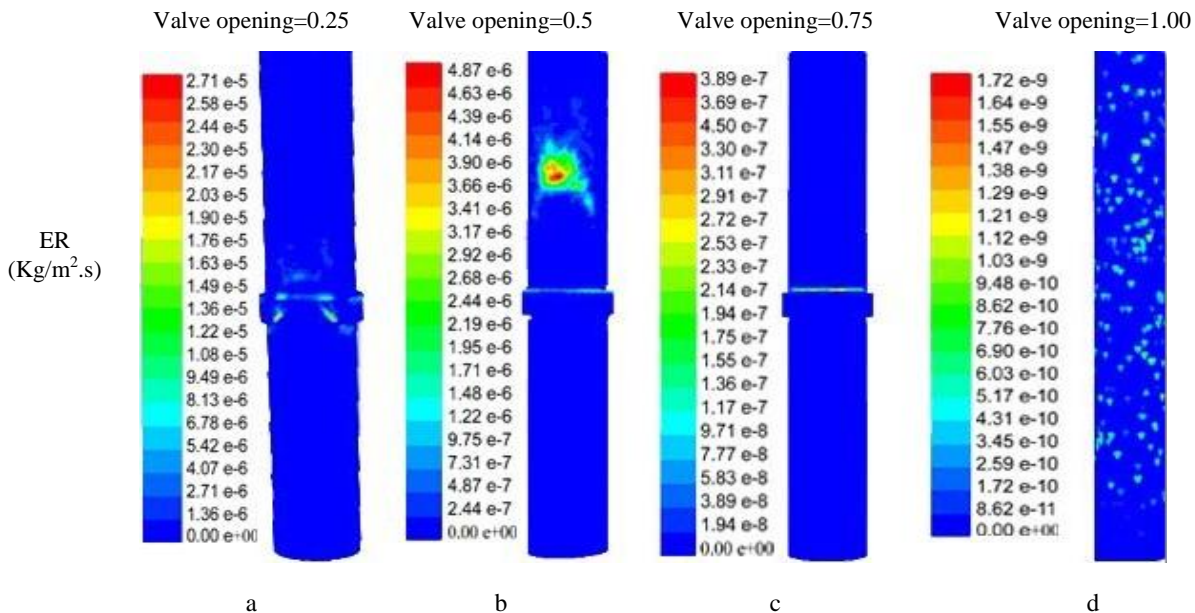


Figure.5. Effects of valve opening on ER for 3% of particle concentration

5.1.3. Particle concentration: 9%

Investigating the results of each state by standard condition that is complete open state of valve is as follows (figure 7):

- In the 25% open state, rate of erosion is increased to 15200.
- In the 50% open state, rate of erosion is increased to 3980.
- In the 75% open state, rate of erosion is increased to 206.

The results are the same as previous steps in terms of kind and place of erosion. But regarding increase in concentration of particles, rate of erosion is increased.

Results. With regard to obtained results it can be said that rate of erosion is increased with change in ball condition of valve and its limitation.

5.2. Effect of change in Concentration of Particles

In this section (figure 8), we investigate output results of four ball conditions (25%, 50%, 75% and 100%) in three different particle concentrations (3%, 6% and 9%).

For every four ball states, it is observed that the rate of erosion is increased when concentration of particles is increased (in three steps of change in particle concentration).

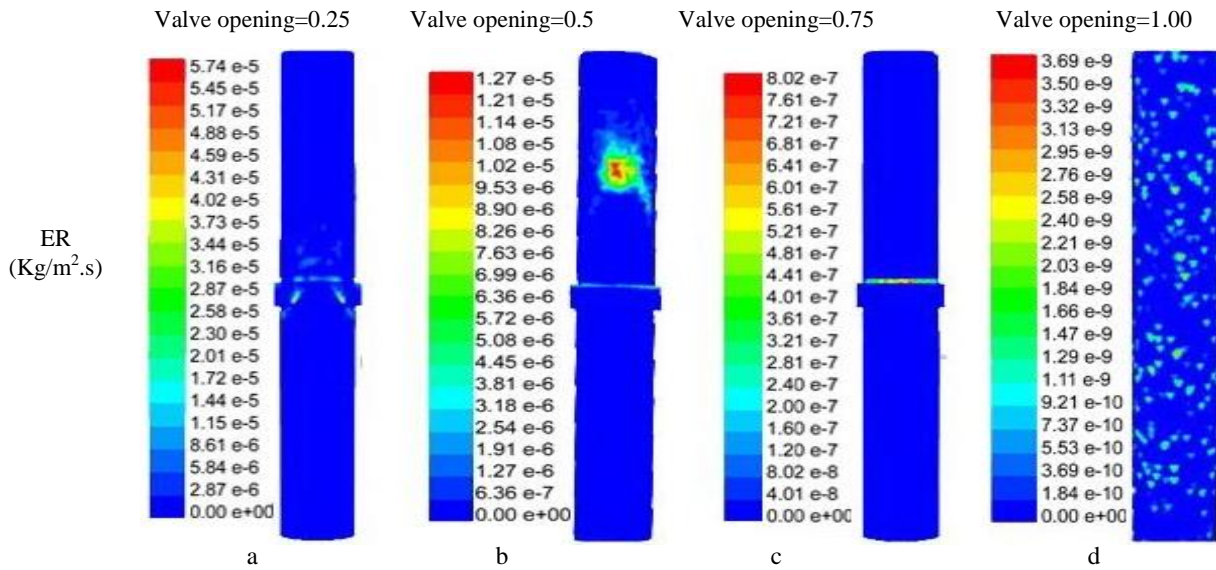


Figure.6. Effects of valve opening on ER for 6% of particle concentration

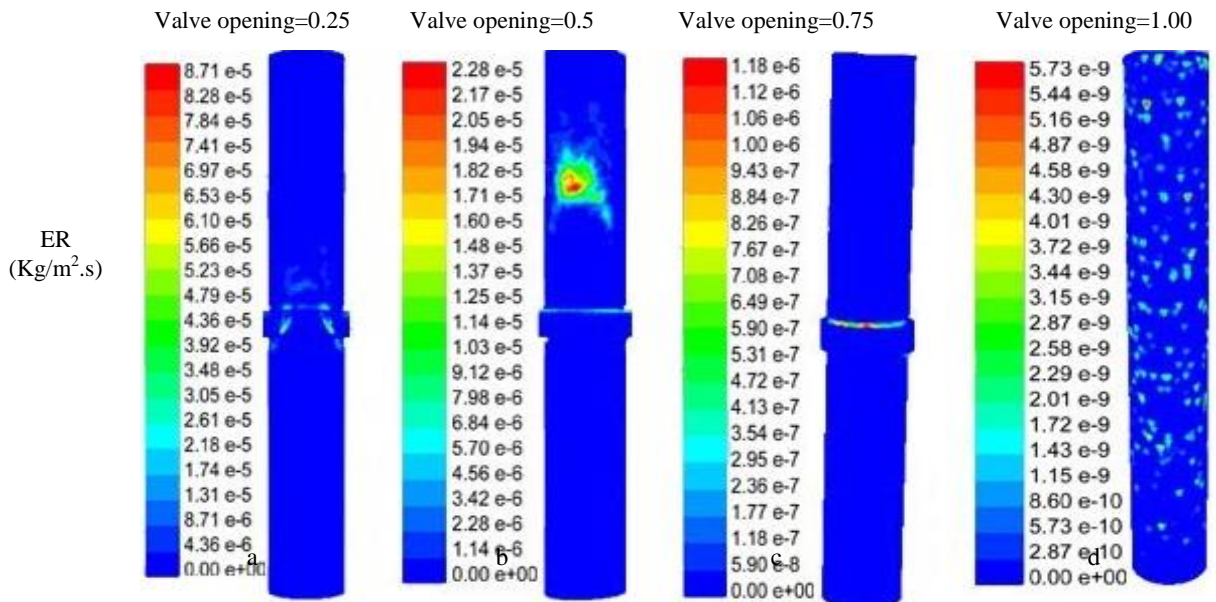


Figure.7. Effects of valve opening on ER for 9% of particle concentration

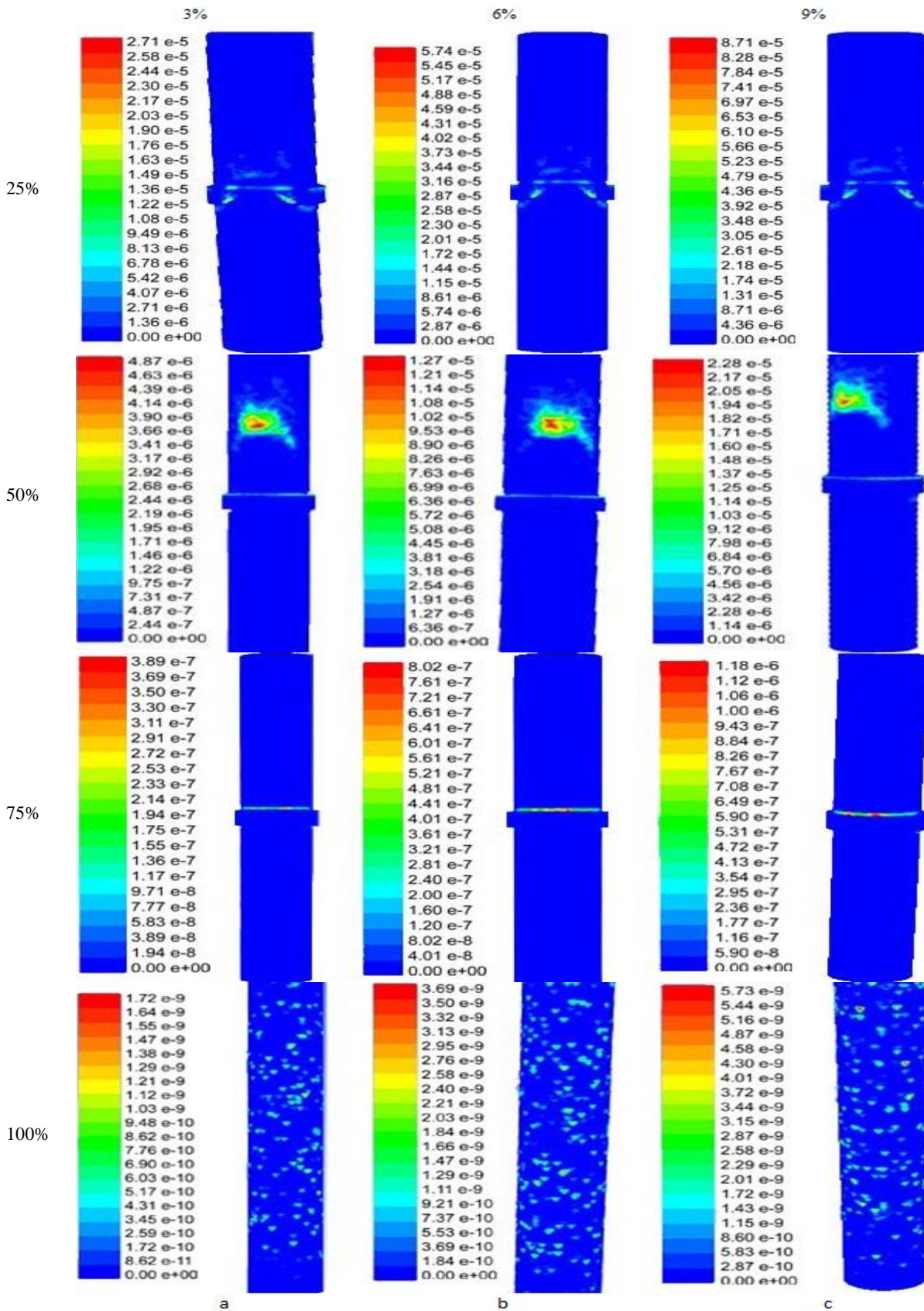


Figure.8. Effects of particle concentration on ER

6. Conclusions

A three-dimensional fluid–structure interaction computational model coupling with a combined continuum and discrete model has been used to predict the erosion rate the flow field distribution of gas particle. flow and the erosion rate of valve

body and core are captured under different operating and structural conditions with different fluid parameters. From the descriptions above, the following conclusions can be drawn :

- 1- If ball valve is used in different conditions, the rate of erosion proportional to complete open state that is standard state of valve is increased very much and its changes are as follow:
- 25% open state of valve is about 15000 times;
 - 50% open state of valve is about 3500 times;
 - 75% open state of valve is about 220 times.
- 2- Rate of erosion is increased when concentration of suspended particles with gas is increased.

References

- [1] K. Haugen, O. Kvernfold, A. Ronold, R. Sandberg, Sand erosion of wear-resistant materials: Erosion in choke valves, *Wear*, Vol. 186, pp. 179-188, 1995.
- [2] B. McLaury, J. Wang, S. Shirazi, J. Shadley, E. Rybicki, Solid particle erosion in long radius elbows and straight pipes, in *Proceeding of, Society of Petroleum Engineers*, pp.
- [3] A. Forder, M. Thew, D. Harrison, A numerical investigation of solid particle erosion experienced within oilfield control valves, *Wear*, Vol. 216, No. 2, pp. 184-193, 1998.
- [4] G. Parslow, D. Stephenson, J. Strutt, S. Tetlow, Investigation of solid particle erosion in components of complex geometry, *Wear*, Vol. 233, pp. 737-745, 1999.
- [5] A. Kavner, T. S. Duffy, G. Shen, Phase stability and density of FeS at high pressures and temperatures: implications for the interior structure of Mars, *Earth and Planetary Science Letters*, Vol. 185, No. 1, pp. 25-33, 2001.
- [6] J. Jin, J. Fan, X. Zhang, K. Cen, Numerical simulation of the tube erosion resulted from particle impacts, *Wear*, Vol. 250, No. 1, pp. 114-119, 2001 .
- [7] J. Fan, K. Luo, X. Zhang, K. Cen, Large eddy simulation of the anti-erosion characteristics of the ribbed-bend in gas-solid flows, *Journal of engineering for gas turbines and power*, Vol. 126, No. 3, pp. 672-679, 2004.
- [8] T. Deng, M. Patel, I. Hutchings, M. Bradley, Effect of bend orientation on life and puncture point location due to solid particle erosion of a high concentration flow in pneumatic conveyors, *Wear*, Vol. 258, No. 1, pp. 426-433, 2005.
- [9] Y. I. Oka, K. Okamura, T. Yoshida, Practical estimation of erosion damage caused by solid particle impact: Part 1: Effects of impact parameters on a predictive equation, *Wear*, Vol. 259, No. 1, pp. 95-101, 2005.
- [10] X. Chen, B. S. McLaury, S. A. Shirazi, Numerical and experimental investigation of the relative erosion severity between plugged tees and elbows in dilute gas/solid two-phase flow, *Wear*, Vol. 261, No. 7, pp. 715-729, 2006.
- [11] M. Habib, H. Badr, S. Said, R. Ben- Mansour, S. Al- Anizi, Solid- particle erosion in the tube end of the tube sheet of a shell- and- tube heat exchanger, *International journal for numerical methods in fluids*, Vol. 50, No. 8, pp. 885-909, 2006.
- [12] R. Malka, S. Nešić, D. A. Gulino, Erosion–corrosion and synergistic effects in disturbed liquid-particle flow, *Wear*, Vol. 262, No. 7, pp. 791-799, 2007.
- [13] M. Suzuki, K. Inaba, M. Yamamoto, Numerical simulation of sand erosion in a square-section 90-degree bend, *Journal of Fluid Science and Technology*, Vol. 3, No. 7, pp. 868-880, 2008.
- [14] P. Tang, J. Yang, J. Zheng, G. Ou, S. He, J. Ye, I. Wong, Y. Ma, Erosion-corrosion failure of REAC pipes under multiphase flow, *Frontiers of Energy and Power Engineering in China*, Vol. 3, No. 4, pp. 389-395, 2009.
- [15] Y. M. Ferng, B. H. Lin, Predicting the wall thinning engendered by erosion–corrosion using CFD methodology, *Nuclear Engineering and Design*, Vol. 240, No. 10, pp. 2836-2841, 2010.
- [16] R. Li, A. Yamaguchi, H. Ninokata, Computational fluid dynamics study of liquid droplet impingement erosion in the inner wall of a bent pipe, *Journal of Power and Energy Systems*, Vol. 4, No. 2, pp. 327-336, 2010.
- [17] B. Yan, H. Gu, L. Yu, CFD analysis of the loss coefficient for a 90° bend in rolling motion, *Progress in Nuclear Energy*, Vol. 56, pp. 1-6, 2012.
- [18] H. Zhang, Y. Tan, D. Yang, F. X. Trias, S. Jiang, Y. Sheng, A. Oliva, Numerical investigation of the location of maximum erosive wear damage in elbow: Effect of slurry velocity, bend orientation and angle of elbow, *Powder Technology*, Vol. 217, pp. 467-476, 2012.
- [19] M. Shahbazi, S. Noori zadeh, Identification of Black Powder in Natural Gas Transmission Network, in *The third scientific conference on process engineering (oil, gas refining and petrochemicals)*, Tehran, 2014. “(in Persian)”
- [20] D. SHAFEE, K. KHORSHIDI, K. M. MORAVEJI, Numerical Analysis of Erosion/Corrosion due to Gas Flow in Pipelines and Gas Stations, 2014. “(in Persian)”
- [21] H. Zhu, Q. Pan, W. Zhang, G. Feng, X. Li, CFD simulations of flow erosion and flow-induced deformation of needle valve: Effects of operation, structure and fluid parameters, *Nuclear Engineering and Design*, Vol. 273, pp. 396-411, 2014.
- [22] M. Droubi, R. Tebowei, S. Islam, M. Hossain, E. Mitchell, *Computational Fluid Dynamic Analysis of Sand Erosion in 90o Sharp Bend Geometry*, 2016.